Horizontal motion in elastic response to seasonal loading of rain water in the Amazon Basin and monsoon water in Southeast Asia observed by GPS and inferred from GRACE

Yuning Fu,[1] Donald F. Argus,[1] Jeffrey T. Freymueller,[2] and Michael B. Heflin[1]

Received 23 September 2013; revised 11 November 2013; accepted 17 November 2013; published 4 December 2013.

[1] We find seasonal horizontal crustal motions observed by GPS positioning in elastic response to heavy rainfall in the Amazon Basin and to monsoons in Southeast Asia to be consistent with those inferred from Gravity Recovery and Climate Experiment (GRACE) gravity observations of water mass loading. Solid Earth moves toward the Amazon during heavy spring rainfall and toward Southeast Asia during summer monsoons and back away from these areas 6 months later when the water load is minimum. Vertical oscillations observed by GPS and inferred from GRACE are 2 to 3 times larger than horizontal oscillation near the margins of the areas of large mass loading. Some discrepancies between GPS and GRACE are probably caused by local effects that influence GPS measurements, because the GPS sites that show significant discrepancies also do not match nearby GPS sites. However, when the load is short wavelength, the limited spatial resolution of GRACE can cause systematic misfits. **Citation:** Fu, Y., D. F. Argus, J. T. Freymueller, and M. B. Heflin (2013), Horizontal motion in elastic response to seasonal loading of rain water in the Amazon Basin and monsoon water in Southeast Asia observed by GPS and inferred from GRACE, *Geophys. Res. Lett.*, *40*, 6048–6053, doi:10.1002/2013GL058093.

1. Introduction

[2] Seasonal hydrological effects are the main cause of global seasonal mass variations. Large-scale seasonal mass movements cause periodic crustal deformation. Modern space geodetic measurements can quantify both hydrological mass variations with the Gravity Recovery and Climate Experiment (GRACE) and loading deformation with the Global Positioning System (GPS).

[3] GPS-observed vertical seasonal oscillations have been studied and compared with GRACE-modeled seasonal loading deformation globally [*Davis et al*., 2004; *Tregoning et al*., 2009; *Tesmer et al*., 2011] and locally for Europe [*van Dam et al*., 2007], Greenland [*Khan et al*., 2010], Nepal Himalaya [*Fu and Freymueller*, 2012], West Africa [*Nahmani et al*., 2012], and southern Alaska [*Fu et al*., 2012]. Consistency between the two techniques' observations of vertical seasonal ground oscillations has been recognized in regions where large-scale seasonal loads are significant and local effects are small.

[4] Most of the studies focused on the vertical component because of its large amplitude. *Wahr et al*. [2013] demonstrated that horizontal displacements are valuable in that they constrain the location of load changes and therefore augment vertical observations [*Nielsen et al*., 2013]. *Tregoning et al*. [2009] indicated correlations of horizontal seasonal deformation between GPS and GRACE where hydrological loading is over broad spatial scales. Because both GRACE and GPS data have been improved compared to earlier date and more continuous GPS stations have been installed, in this study we investigate horizontal seasonal deformations in the two areas with the largest seasonal mass variations in the world: the Amazon River Basin and Southeast Asia. We furthermore evaluate the consistency between these two geodetic measurements using an elastic loading model.

2. Geodetic Measurements

2.1. GPS Data and Processing

[5] GPS data analysis was performed with Jet Propulsion Laboratory's (JPL's) GPS Inferred Positioning System (GIPSY) software version 6.2 in Precise Point Positioning mode [*Zumberge et al*., 1997]. JPL's reanalysis orbits and clocks are based on upgraded models including the DE421 planetary ephemeris, the GSPM10 satellite solar pressure model, the IAU06 precession and nutation model, IERS2010 tides, the FES2004 ocean loading model, and the use of International GNSS Service (IGS) satellite and receiver phase center maps [*Desai et al*., 2009]. The Vienna Mapping Function 1 [*Boehm et al*., 2006; *Kouba*, 2008] is adopted, and GPS positions are transformed into the IGS08 frame, the IGS realization of ITRF2008. We correct atmospheric loading displacement using data provided by the Global Geophysical Fluid Center [*van Dam and Wahr*, 1987; *van Dam*, 2010]. We average atmospheric loading into monthly corrections and remove them from monthly averaged GPS solutions. In order to investigate the seasonal movement, GPS time series are detrended, and tectonic movements are therefore removed. More information about the GPS data processing is provided in the supporting information.

2.2. GRACE Data and Its Modeled Horizontal Deformation

[6] We use the GRACE Level-2 RL05 solution from Center for Space Research (Austin, U.S.) for our study. The time-variable spherical harmonic coefficients (up to degree

Additional supporting information may be found in the online version of this article.

[1]Jet Propulsion Laboratory, California Institute of Technology, Pasadena, California, USA.
[2]Geophysical Institute, University of Alaska Fairbanks, Fairbanks, Alaska, USA.

Corresponding author: Y. Fu, Jet Propulsion Laboratory, California Institute of Technology, Pasadena, CA 91109, USA. (Yuning.Fu@jpl.nasa.gov)

0094-8276/13/10.1002/2013GL058093

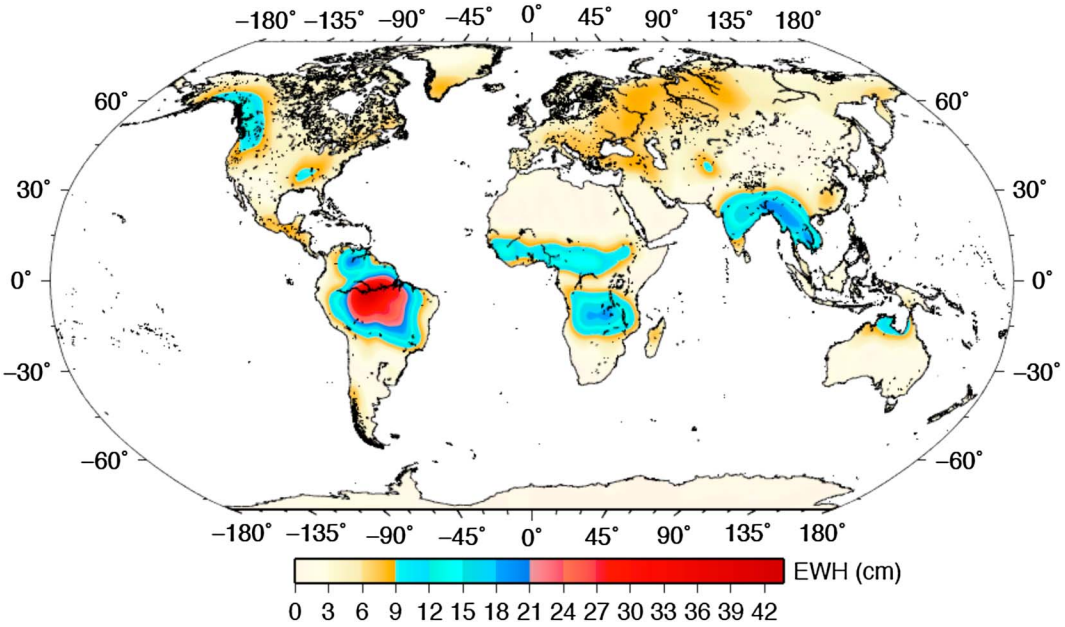

Figure 1. Amplitude of global seasonal mass variation in terms of equivalent water height (EWH) measured by GRACE.

and order 60) of the Earth's gravity field are used to model the lithosphere elastic displacement due to the changing surface mass load [*Kusche and Schrama*, 2005].

$$\Delta e = \frac{R}{\sin\theta}\sum_{l=1}^{\infty}\sum_{m=0}^{l}\overline{P}_{lm}(\cos\theta)\cdot m\cdot\left[-\Delta\overline{C}_{lm}\sin(m\phi)+\Delta\overline{S}_{lm}\cos(m\phi)\right]\cdot\frac{l'_l}{1+k'_l}$$

$$\Delta n = -R\sum_{l=1}^{\infty}\sum_{m=0}^{l}\frac{\partial}{\partial\theta}\overline{P}_{lm}(\cos\theta)\cdot\left[\Delta\overline{C}_{lm}\cos(m\phi)+\Delta\overline{S}_{lm}\sin(m\phi)\right]\cdot\frac{l'_l}{1+k'_l}$$

$$\Delta h = R\sum_{l=1}^{\infty}\sum_{m=0}^{l}\overline{P}_{lm}(\cos\theta)\cdot\left[\Delta\overline{C}_{lm}\cos(m\phi)+\Delta\overline{S}_{lm}\sin(m\phi)\right]\cdot\frac{h'_l}{1+k'_l} \quad (1)$$

where R is the Earth's radius; θ and ϕ are colatitude and longitude; $\overline{P}_{lm}$ are normalized associated Legendre functions for degree l and order m; $\Delta\overline{C}_{lm}$ and $\Delta\overline{S}_{lm}$ are spherical harmonic coefficients of the time-variable Earth's gravity field relative to a long-term average; and l'_l, h'_l, and k'_l are the load Love numbers at degree l. In this study, we adopt load Love numbers provided by *Farrell* [1972], which are computed relative to the center of mass of solid earth. Farrell's load Love numbers are based on the Gutenberg-Bullen Earth model. We compared this with the result using load Love numbers based on the Preliminary Reference Earth Model (PREM), and the difference is very small and can be neglected.

[7] Because GRACE cannot determine degree 1 variations, and GRACE by itself cannot accurately determine the C20 term, we change the degree 1 terms to those provided by *Swenson et al*. [2008] and also replace the GRACE C20 component using the results from Satellite Laser Ranging measurements [*Cheng and Tapley*, 2004]. We use 350 km as the averaging radius for Gaussian smoothing to suppress errors at higher degrees [*Wahr et al*., 1998].

3. Study Areas

[8] Figure 1 shows the global seasonal mass variation measured by GRACE in terms of equivalent water height. We fit GRACE-measured mass variation time series (from January 2003 to December 2012) with linear and seasonal annual components, and then evaluate the annual amplitude. Figure 1 clearly shows the regions with great large-scale seasonal mass oscillations. The two regions with the most significant seasonal mass cycles are the Amazon Basin and Southeast Asia. In this paper, we use GPS and GRACE to investigate horizontal crustal seasonal deformation in these two regions.

3.1. Amazon Basin

[9] The Amazon River Basin has the world's largest continental seasonal water variations (Figure 1) and is critical to Earth's hydrological system, including the exchange of water between the Amazon rainforest, the oceans, and the atmosphere [*Gloor et al*., 2013]. Interannual variations in Amazon rainfall, such as years of light and heavy rain, have been evaluated using GRACE [*Chen et al*., 2010]. Solid Earth's elastic seasonal response to oscillations of Amazon water has been analyzed using GPS [*Bevis et al*., 2005] and compared with GRACE-modeled results [*Davis et al*., 2004]. In this study, we combine GPS and GRACE to assess the crustal horizontal seasonal deformation in the Amazon Basin.

[10] Figure 2 shows examples of both GPS-measured and GRACE-modeled (with equation (1)) horizontal crustal seasonal (detrended) variations. It is clear that GPS and GRACE record coherent horizontal ground seasonal movements. The good correlation between these two geodetic measurements confirms that the seasonal crustal deformation is caused by the hydrological seasonal mass loading variations and that both GPS and GRACE can resolve this horizontal seasonal deformation. We also plot the seasonal displacement time series in height in Figure S1, which also shows good correlation.

[11] To characterize the horizontal crustal oscillations, we define and derive "seasonal vectors" as follows: first, we fit the GPS (or GRACE) time series with linear and seasonal terms (GPS time series may also require the estimation of offsets caused by identified equipment changes and earthquakes, whereas GRACE time series do not), then we estimate the time when the height time series reaches its

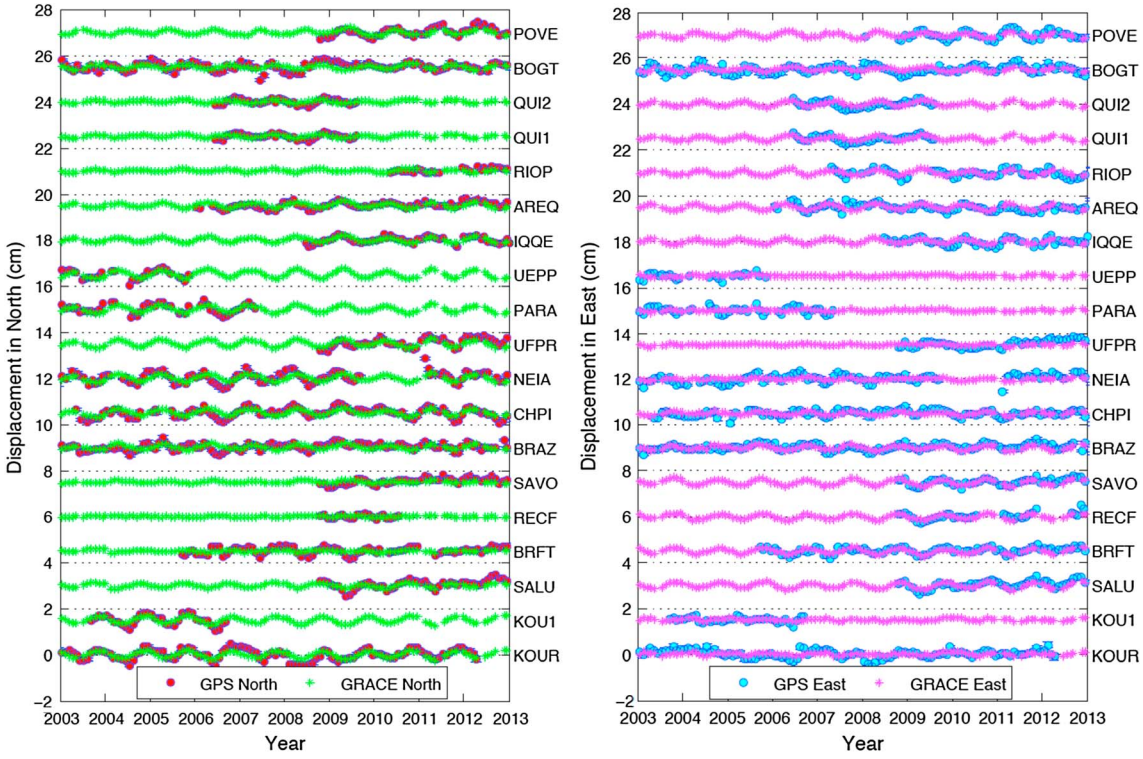

Figure 2. Ground horizontal seasonal deformation (north and east components) measured by GPS and modeled by GRACE in the Amazon Basin.

highest peak; this is also the time when the surface load is minimum. Then we calculate the seasonal displacements (peak-to-peak amplitude) for the horizontal (north and east) directions. Figure 3 (left) gives an example (GPS station SALU) of the strategy we use to derive the seasonal vector. The vector represents the north and east components of the peak-to-peak seasonal displacements. In theory, the ground should move away from the load at this time because the load is minimum.

[12] Figure 3 (right) shows the seasonal vectors for both GPS-measured and GRACE-modeled seasonal crustal horizontal and vertical deformation around the Amazon Basin. The peak-to-peak horizontal amplitude can reach several millimeters (Figure 3, right). It clearly indicates that the ground moves away from the load when the load is minimum, exactly as predicted by the elastic loading theory. Because the GPS stations used in this study are well distributed around the Amazon Basin, the directions (or azimuths)

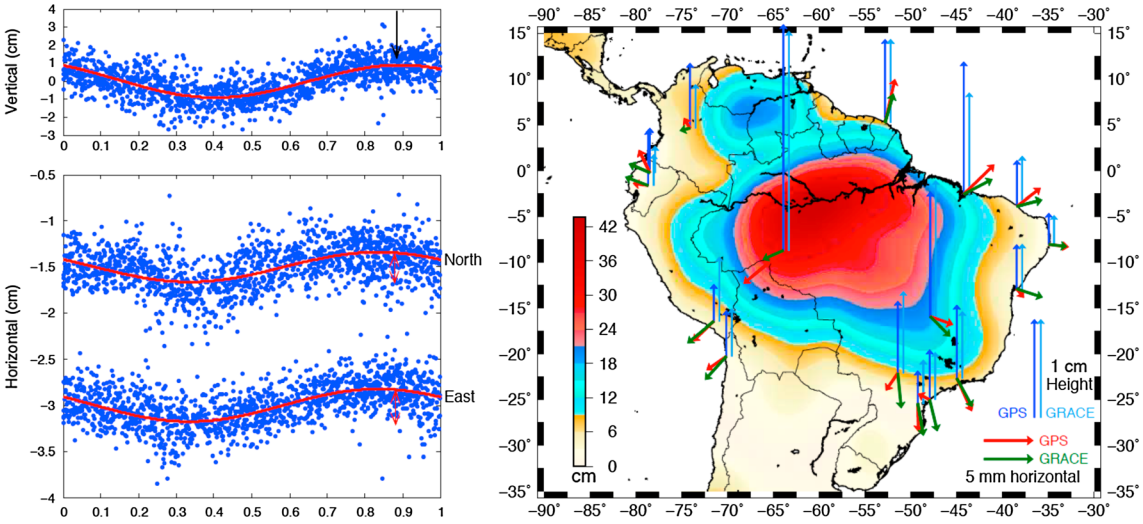

Figure 3. (left) An example (GPS station SALU) of the strategy we use to derive the seasonal vector. (right) Horizontal seasonal vectors (peak-to-peak amplitude) for stations around the Amazon Basin; red and green are GPS-measured and GRACE-modeled horizontal seasonal vector individually; blue and light blue are for the vertical component. The background color indicates amplitude of seasonal mass variations in terms of equivalent water height, with the same color scale as in Figure 1.

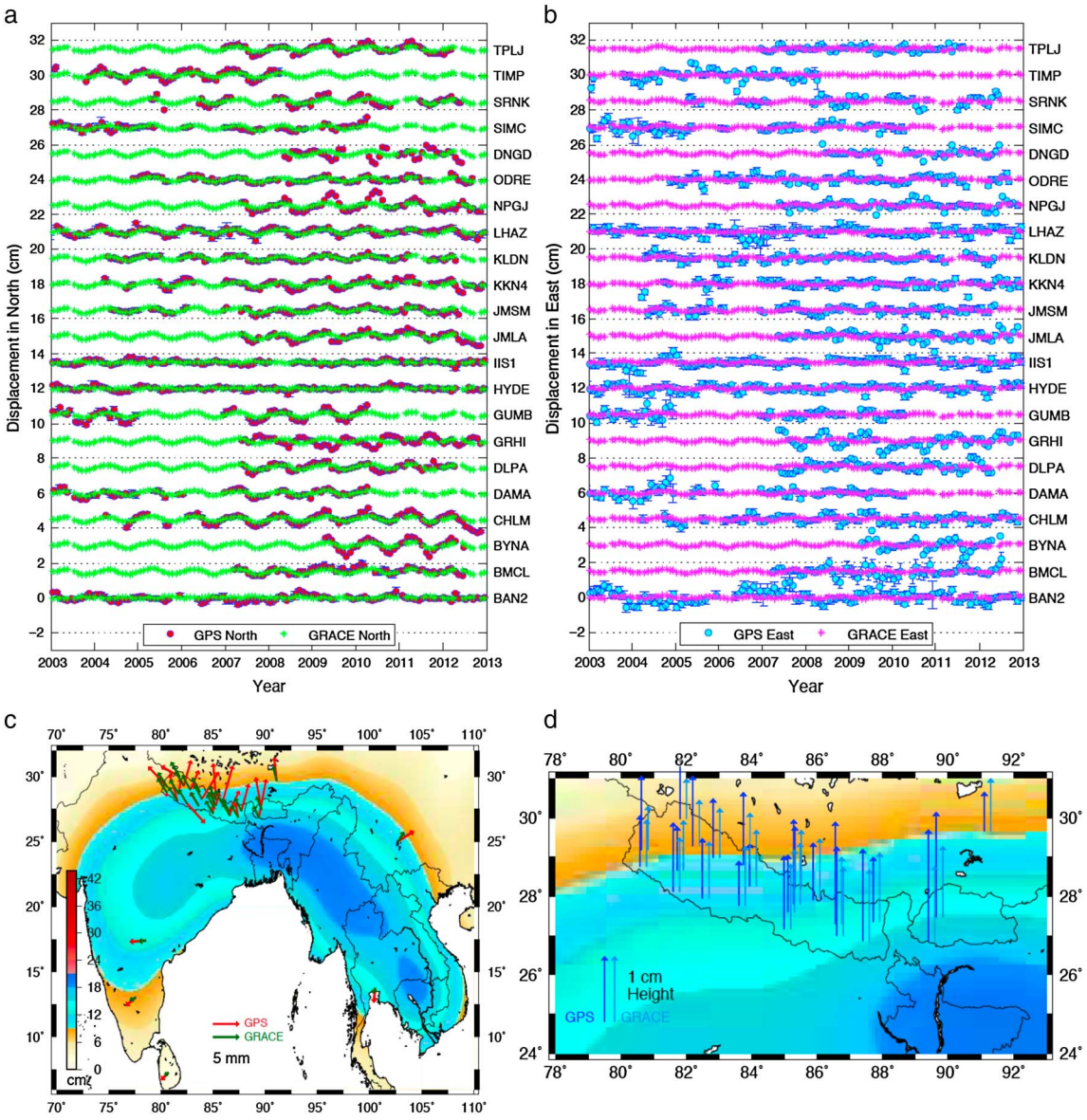

Figure 4. Results for Southeast Asia: (a. b) example time series of GPS-measured and GRACE-modeled horizontal seasonal deformation; (c) seasonal vector for horizontal component in Southeast Asia and the (d) vertical component in Nepal. The background color indicates the amplitude of seasonal mass variations in terms of equivalent water height, with the same color scale as in Figure 1.

of the seasonal vectors match the shape of load. The vertical component also exhibits good correlation between GPS and GRACE. The vertical oscillations observed by GPS and inferred from GRACE are 2 to 3 times larger than horizontal oscillation near the margins of the areas of large mass loading, consistent with *Wahr et al*. [2013].

[13] We also adopt the WRMS (Weighted Root-Mean-Squares) reduction ratio [*Fu et al*., 2012] to assess their correlations between GPS-measured and GRACE-modeled horizontal seasonal deformation (Figure S2). Our analysis indicates that for the GPS stations located west and east of the load, such as QUI1, QUI2, RIOP, RECF, BRAZ, and SAVO, the correlation is good in the east direction and poor in the north direction. This is because their horizontal seasonal movements are mainly in the east-west direction. For the stations on the south side of the load, such as UFPR, CHPI, and UEPF, the correlations in the north component are much better than those in the east component. The values of WRMS reduction ratio for all the stations are provided and plotted in Table S1 and Figure S2.

3.2. Southeast Asia

[14] The South Asia monsoon brings significant water mass load during the summer season from June through September. The high Himalaya range blocks the northward moisture-rich monsoon winds, so that moist air is raised in altitude and cooled in temperature, which results in strong precipitation. The seasonal mass variation in Southeast Asia is the second largest globally, smaller only than the Amazon Basin (Figure 1). *Steckler et al*. [2010] used GPS height oscillations to study the hydrology-induced seasonal ground vertical deformation in Bangladesh. *Fu and Freymueller* [2012] investigated the vertical seasonal deformation in the Nepal Himalaya with GPS and GRACE measurements. *Bettinelli*

et al. [2008] found that the Southeast Asia monsoon water load produces seasonal oscillations of the north component of GPS sites in the Nepal Himalaya, as well as seasonal stress variations there recorded in seismicity rates.

[15] Because *Fu and Freymueller* [2012] systematically analyzed the vertical seasonal hydrological loading in this region, here we mainly study the horizontal seasonal loading deformation using the continuous GPS stations installed in Nepal (north of the monsoon load) and several other IGS GPS stations. Figures 4a and 4b show examples of GPS-measured and GRACE-modeled crustal horizontal seasonal deformations and their time series in height are shown in Figure S3. It is clear that the coherence in north is better than that of east component. The reason is given below.

[16] With the same strategy as illustrated in Figure 3, we derive and plot the horizontal seasonal vector in Figure 4c. Both GPS and GRACE indicate the crust moves away from the load when the load is minimum. For the stations in Nepal, north of the seasonal monsoon load, the seasonal vectors mostly point to the north. For the stations in southern India (IISC, BAN2, and IISC) and Sri Lanka (PALK), the seasonal vectors point to southwest, and for the site KUNM (Kunming, China), the seasonal vector points to the northeast, because of their locations relative to the load (see Figure 4c). The seasonal vertical movements for GPS and GRACE in Nepal are also shown (Figure 4d).

[17] Analysis of the WRMS reduction ratio for stations in Nepal clearly shows that the correlations between GPS-measured and GRACE-modeled seasonal deformation in the north direction are better than that in east (Figure S4 and Table S2). That is because the seasonal monsoon load is located south of Nepal, and the horizontal seasonal movement is mainly in the north-south direction; predicted east-west seasonal motions are very small.

4. Discussion

[18] While the seasonal hydrological loading deformation is more significant in the vertical component [*Tesmer et al*., 2011], our study demonstrates that GPS and GRACE both can resolve seasonal horizontal deformation caused by large-scale loading [*Tregoning et al*., 2009], including the hydrological cycle in the Amazon Basin and the summer monsoon in Southeast Asia. These horizontal seasonal motions can exceed 5 mm peak to peak for the seasonal loads considered in this paper.

[19] Due to its limited spatial resolution, GRACE can only resolve long-wavelength mass load variations. GPS is also sensitive to short-wavelength loading changes. GPS is more likely influenced by local effects, such as local site instability or compaction and decompaction associated with aquifer drawdown and recharge [e.g., *Bawden et al*., 2001]. Therefore our GPS solutions show higher scatter than the GRACE (Figures 3 and 4). We also find a few mismatches in the seasonal vectors. In southwest Nepal, two GPS stations, DNGD (Dhangadi) and GRHI (Ghorahi), show opposite horizontal seasonal movement directions to the GRACE modeled results. The horizontal seasonal motions of these sites are also out of phase with nearby GPS sites, which suggests a local cause. DNGD (Dhangadi, Nepal) is surrounded by farmlands and is probably influenced by local groundwater irrigation [*Shah et al*., 2006]. GRHI (Ghorahi, Nepal) is located on the southern edge of the Dang Valley, Nepal. We suspect the horizontal movement of GRHI is dominated by the local effect of the valley. There is a more systematic orientation difference between the directions of the seasonal vectors for sites in northern Nepal and for all sites in eastern Nepal. This could be a result of spatial smoothing in the GRACE solutions, because the pattern of the largest part of the load is likely to be narrow in the north-south direction, following the Ganges valley. The GPS seasonal vectors are more consistent with a river load that is more uniform along the Ganges River adjacent to central and eastern Nepal than the GRACE estimate.

[20] Our results indicate the agreement of GPS and GRACE in the Amazon is generally better than that of southeast Asia, as noted by *Tregoning et al*. [2009]. However, in both places we find better agreement between GPS and GRACE than that of earlier studies, likely reflecting the greater amount of data and model improvements made since that time. Our results indicate that large-scale hydrological loading is the main factor affecting seasonal deformation in the Amazon Basin; the magnitude of seasonal mass variation is larger than that of Southeast Asia and local effects are smaller. In Southeast Asia, although the horizontal seasonal displacements correlate with their locations relative to the load, the misfit between the two estimates is larger, due to the shorter spatial wavelength of the load and a few sites with local effects in the GPS data.

[21] Other studies have also found scale differences between GPS-measured and GRACE-modeled loading deformation. For example, *Khan et al*. [2010] estimated a scale factor of ~2.5 between GPS and GRACE vertical deformations in Greenland, due to the fact that short-wavelength loads dominate the signal there, in that case due to ice loss from coastal glaciers and ice fields close to the GPS stations. GRACE, on the other hand, can only sense a long-wavelength average of the load, which produces a broader but lower amplitude vertical deformation field. For the two regions studied in this paper, the scale factors are 1.04 ± 0.42 for horizontal direction and 1.11 ± 0.32 for vertical component in the Amazon, and 1.59 ± 0.62 for horizontal and 1.22 ± 0.44 for vertical in Southeast Asia, indicating that the scale factor may contain information about the dominant wavelength and proximity of the load.

5. Conclusions

[22] We find that both GPS and GRACE can resolve large-scale horizontal seasonal loading deformation. Comparison between GPS-measured and GRACE-modeled seasonal horizontal deformation in the Amazon Basin and Southeast Asia indicates good correlation for the seasonal horizontal movements. This indicates that GPS horizontal displacements may be used to constrain the location and size of mass. However, GPS measurement can be sensitive to local effects, and may include other signals rather than large-scale loading, and GRACE estimates are limited when the dominant wavelength of the load becomes too short.

[23] **Acknowledgments.** We greatly appreciate Jean-Philippe Avouac and his group at Caltech Tectonics Observatory for maintaining continuous GPS measurements in Nepal. YF thanks Richard Gross and Susan Owen for helpful discussion. We are grateful to Paul Tregoning, Shfaqat Abbas Khan, and an anonymous reviewer for constructive criticism and comments that significantly improve the manuscript. YF was supported through the NASA Postdoctoral Program at Jet Propulsion Laboratory. This paper presents the results carried out at the Jet Propulsion Laboratory, California Institute of Technology, sponsored by the National Aeronautics and Space Administration (NASA).

[24] The Editor thanks Paul Tregoning and an anonymous reviewer for their assistance in evaluating this paper.

References

Bawden, G. W., W. Thatcher, R. S. Stein, K. W. Hudnut, and G. Peltzer (2001), Tectonic contraction across Los Angeles after removal of groundwater pumping effects, *Nature*, *412*, 812–815.

Bettinelli, P., J.-P. Avouac, M. Flouzat, L. Bollinger, G. Ramillien, S. Rajaure, and S. Sapkota (2008), Seasonal variations of seismicity and geodetic strain in the Himalaya induced by surface hydrology, *Earth Planet. Sci. Lett.*, *266*, 332–344, doi:10.1016/j.epsl.2007.11.021.

Bevis, M., D. Alsdorf, E. Kendrick, L. P. Fortes, B. Forsberg, R. Smalley Jr., and J. Becker (2005), Seasonal fluctuations in the mass of the Amazon River system and Earth's elastic response, *Geophys. Res. Lett.*, *32*, L16308, doi:10.1029/2005GL023491.

Boehm, J., B. Werl, and H. Schuh (2006), Troposphere mapping functions for GPS and very long baseline interferometry from European Centre for Medium-Range Weather Forecasts operational analysis data, *J. Geophys. Res.*, *111*, B02406, doi:10.1029/2005JB003629.

Chen, J. L., C. R. Wilson, and B. D. Tapley (2010), The 2009 exceptional Amazon flood and interannual terrestrial water storage change observed by GRACE, *Water Resour. Res.*, *46*, W12526, doi:10.1029/2010WR009383.

Cheng, M., and B. D. Tapley (2004), Variations in the Earth's oblateness during the past 28 years, *J. Geophys. Res.*, *109*, B09402, doi:10.1029/2004JB003028.

Davis, J. L., P. Elósegui, J. X. Mitrovica, and M. E. Tamisiea (2004), Climate-driven deformation of the solid Earth from GRACE and GPS, *Geophys. Res. Lett.*, *31*, L24605, doi:10.1029/2004GL021435.

Desai, S., W. Bertiger, B. Haines, N. Harvey, D. Kuang, C. Lane, A. Sibthorpe, F. Webb, and J. Weiss (2009), The JPL IGS analysis center: Results from the reanalysis of the global GPS network, *Eos Trans. AGU*, *90*(52), Fall Meet. Suppl., Abstract G11B-030.

Farrell, W. E. (1972), Deformation of the Earth by surface loads, *Rev. Geophys. Space Phys.*, *10*, 761–797, doi:10.1029/RG010i003p00761.

Fu, Y., and J. T. Freymueller (2012), Seasonal and long-term vertical deformation in the Nepal Himalaya constrained by GPS and GRACE measurements, *J. Geophys. Res.*, *117*, B03407, doi:10.1029/2011JB008925.

Fu, Y., J. T. Freymueller, and T. Jensen (2012), Seasonal hydrological loading in southern Alaska observed by GPS and GRACE, *Geophys. Res. Lett.*, *39*, L15310, doi:10.1029/2012GL052453.

Gloor, M., R. J. W. Brienen, D. Galbraith, T. R. Feldpausch, J. Schöngart, J.-L. Guyot, J. C. Espinoza, J. Lloyd, and O. L. Phillips (2013), Intensification of the Amazon hydrological cycle over the last two decades, *Geophys. Res. Lett.*, *40*, 1729–1733, doi:10.1002/grl.50377.

Khan, S. A., J. Wahr, M. Bevis, I. Velicogna, and E. Kendrick (2010), Spread of ice mass loss into northwest Greenland observed by GRACE and GPS, *Geophys. Res. Lett.*, *37*, L06501, doi:10.1029/2010GL042460.

Kouba, J. (2008), Implementation and testing of the gridded Vienna Mapping Function 1 (VMF1), *J. Geod.*, *82*, 193–205, doi:10.1007/s00190-007-0170-0.

Kusche, J., and E. J. O. Schrama (2005), Surface mass redistribution inversion from global GPS deformation and Gravity Recovery and Climate Experiment (GRACE) gravity data, *J. Geophys. Res.*, *110*, B09409, doi:10.1029/2004JB003556.

Nahmani, S., et al. (2012), Hydrological deformation induced by the West African Monsoon: Comparison of GPS, GRACE and loading models, *J. Geophys. Res.*, *117*, B05409, doi:10.1029/2011JB009102.

Nielsen, K., S. A. Khan, G. Spada, J. Wahr, M. Bevis, L. Liu, and T. van Dam (2013), Vertical and horizontal surface displacements near Jakobshavn Isbræ driven by melt-induced and dynamic ice loss, *J. Geophys. Res. Solid Earth*, *118*, 1837–1844, doi:10.1002/jgrb.50145.

Shah, T., O. P. Singh, and A. Mukherji (2006), Some aspects of South Asia's groundwater irrigation economy: Analyses from a survey in India, Pakistan, Nepal Terai and Bangladesh, *Hydrogeol. J.*, *14*, 286–309, doi:10.1007/s10040-005-0004-1.

Steckler, M. S., S. L. Nooner, S. H. Akhter, S. K. Chowdhury, S. Bettadpur, L. Seeber, and M. G. Kogan (2010), Modeling Earth deformation from monsoonal flooding in Bangladesh using hydrographic, GPS, and Gravity Recovery and Climate Experiment (GRACE) data, *J. Geophys. Res.*, *115*, B08407, doi:10.1029/2009JB007018.

Swenson, S., D. Chambers, and J. Wahr (2008), Estimating geocenter variations from a combination of GRACE and ocean model output, *J. Geophys. Res.*, *113*, B08410, doi:10.1029/2007JB005338.

Tesmer, V., P. Steigenberger, T. van Dam, and T. Mayer-Gürr (2011), Vertical deformations from homogeneously processed GRACE and global GPS long-term series, *J. Geod.*, *85*, 291–310, doi:10.1007/s00190-010-0437-8.

Tregoning, P., C. Watson, G. Ramillien, H. McQueen, and J. Zhang (2009), Detecting hydrologic deformation using GRACE and GPS, *Geophys. Res. Lett.*, *36*, L15401, doi:10.1029/2009GL038718.

van Dam, T. (2010), NCEP Derived 6 hourly, global surface displacements at 2.5X2.5 degree spacing. [Available at http://geophy.uni.lu/ncep-loading.html.]

van Dam, T. M., and J. M. Wahr (1987), Displacements of the Earth's surface due to atmospheric loading: Effects on gravity and baseline measurements, *J. Geophys. Res.*, *92*, 1281–1286.

van Dam, T., J. Wahr, and D. Lavallée (2007), A comparison of annual vertical crustal displacements from GPS and Gravity Recovery and Climate Experiment (GRACE) over Europe, *J. Geophys. Res.*, *112*, B03404, doi:10.1029/2006JB004335.

Wahr, J., M. Molenaar, and F. Bryan (1998), Time variability of the Earth's gravity field: Hydrological and oceanic effects and their possible detection using GRACE, *J. Geophys. Res.*, *103*, 30,205–30,229, doi:10.1029/98JB02844.

Wahr, J., S. A. Khan, T. van Dam, L. Liu, J. H. van Angelen, M. R. van den Broeke, and C. M. Meertens (2013), The use of GPS horizontals for loading studies, with applications to Northern California and southeast Greenland, *J. Geophys. Res. Solid Earth*, *118*, 1795–1806, doi:10.1002/jgrb.50104.

Zumberge, J. F., M. B. Heflin, D. C. Jefferson, M. M. Watkins, and J. F. H. Webb (1997), Precise point positioning for the efficient and robust analysis of GPS data from large networks, *J. Geophys. Res.*, *102*, 5005–5017.